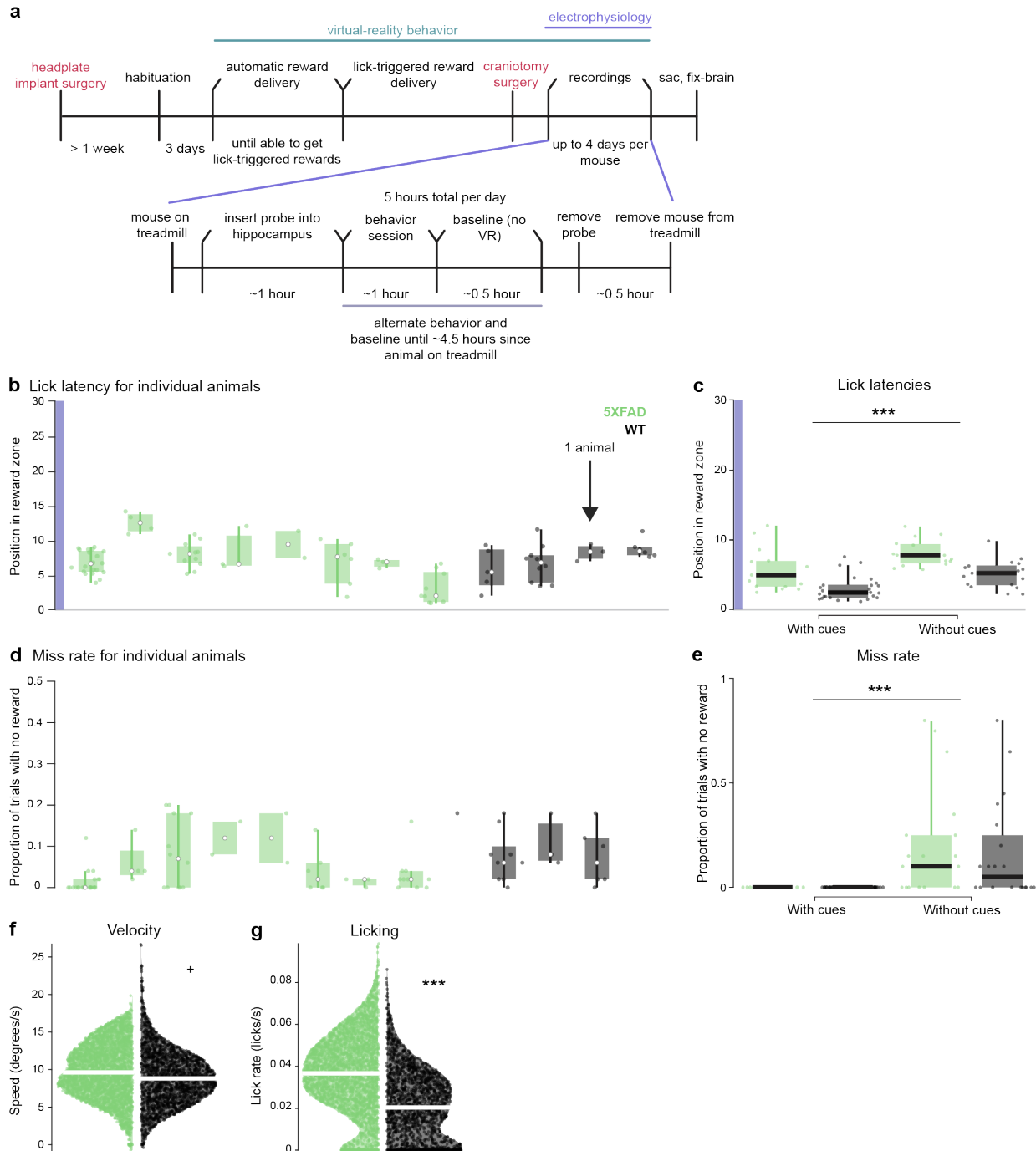


**Cell Reports, Volume 35**

**Supplemental information**

**Alzheimer's pathology causes impaired  
inhibitory connections and reactivation  
of spatial codes during spatial navigation**

**Stephanie M. Prince, Abigail L. Paulson, Nuri Jeong, Lu Zhang, Solange Amigues, and Annabelle C. Singer**



**Figure S1. Experimental timeline and behavioral metrics for individual animals. Related to Figure 1.**

- A.** Timeline of surgeries, behavioral training, and electrophysiological recording sessions.
- B.** Lick latency for 50-trial blocks for individual animals in *5XFAD* (green) and *WT* (black) mice. Purple highlight indicates length of reward zone. Lick latency was only calculated if the animal licked in the reward zone. White dots indicate median value for each animal's distribution, black and green dots indicate 50-trial blocks.
- C.** Lick latency for 50-trial blocks in *5XFAD* (green) and *WT* (black) mice in the track *with visual cues* and the track *without visual cues*. For the comparison between tracks with and without visual cues, six

mice not included in the electrophysiological analysis were trained on the annular track. The last two days of the track with cues and the first two days of the track without cues were used for comparison. Black bar indicates median of distribution. Prob(with cues  $\geq$  without cues)  $< 10^{-4}$  (limit due to resampling  $10^4$  times) \*\*\*. *With cues*: 5XFAD lick latency percentiles: [2.46 3.30 4.95 6.94 12.06], *WT* lick latency percentiles: [1.15 1.68 2.44 3.49 7.58], *without cues*: 5XFAD lick latency percentiles: [5.75 6.75 7.82 9.37 11.96], *WT* lick latency percentiles: [2.21 3.57 5.23 6.28 9.86].

- D. Miss rate (number of laps around the annular track with zero rewards received) for 50-trial blocks for individual animals in 5XFAD (green) and *WT* (black) mice. We observed some outlier trial blocks, and we removed these outliers as described in the **Methods**.
- E. Miss rate for 50-trial-blocks in the annular track *with visual cues* versus the track *without visual cues* in both 5XFAD (green) and *WT* (black) mice. Black bar indicates median of distribution. Prob(with cues  $\geq$  without cues)  $< 10^{-4}$  (limit due to resampling  $10^4$  times) \*\*\*. *With cues*: 5XFAD miss rate percentiles: [0 0 0 0 0], *WT* miss rate percentiles: [0 0 0 0 0], *without cues*: 5XFAD miss rate percentiles: [0 0 0.10 0.25 0.80], *WT* miss rate percentiles: [0 0 0.05 0.23 0.80].
- F. Distribution of velocities (degrees per second) in 5XFAD (green) and *WT* (black) mice. Each data point is the average for a trial, not an entire session. White bar indicates median of distribution. 5XFAD:  $9.77 \pm 0.58$ , *WT*:  $8.98 \pm 0.57$ . Prob(*WT*  $\geq$  5XFAD) = 0.036 +, 5XFAD: degrees per second percentiles = [-0.75 7.18 9.62 12.46 19.85], *WT*: degrees per second percentiles = [-0.39 6.41 8.83 11.32 26.68].
- G. Distribution of licking rates in 5XFAD (green) and *WT* (black) mice. Each data point is the average for a trial, not an entire session. White bar indicates median of distribution. 5XFAD:  $0.036 \pm 0.0028$  Hz, *WT*:  $0.021 \pm 0.0027$ . Prob(*WT*  $\geq$  5XFAD)  $< 10^{-4}$  (limit due to resampling  $10^4$  times) \*\*\*, 5XFAD: lick rate percentiles = [0 0.024 0.037 0.049 0.098], *WT*: lick rate percentiles = [0 0.0045 0.020 0.033 0.086].

All percentiles are min, 25<sup>th</sup> percentile, median, 75<sup>th</sup> percentile, max.

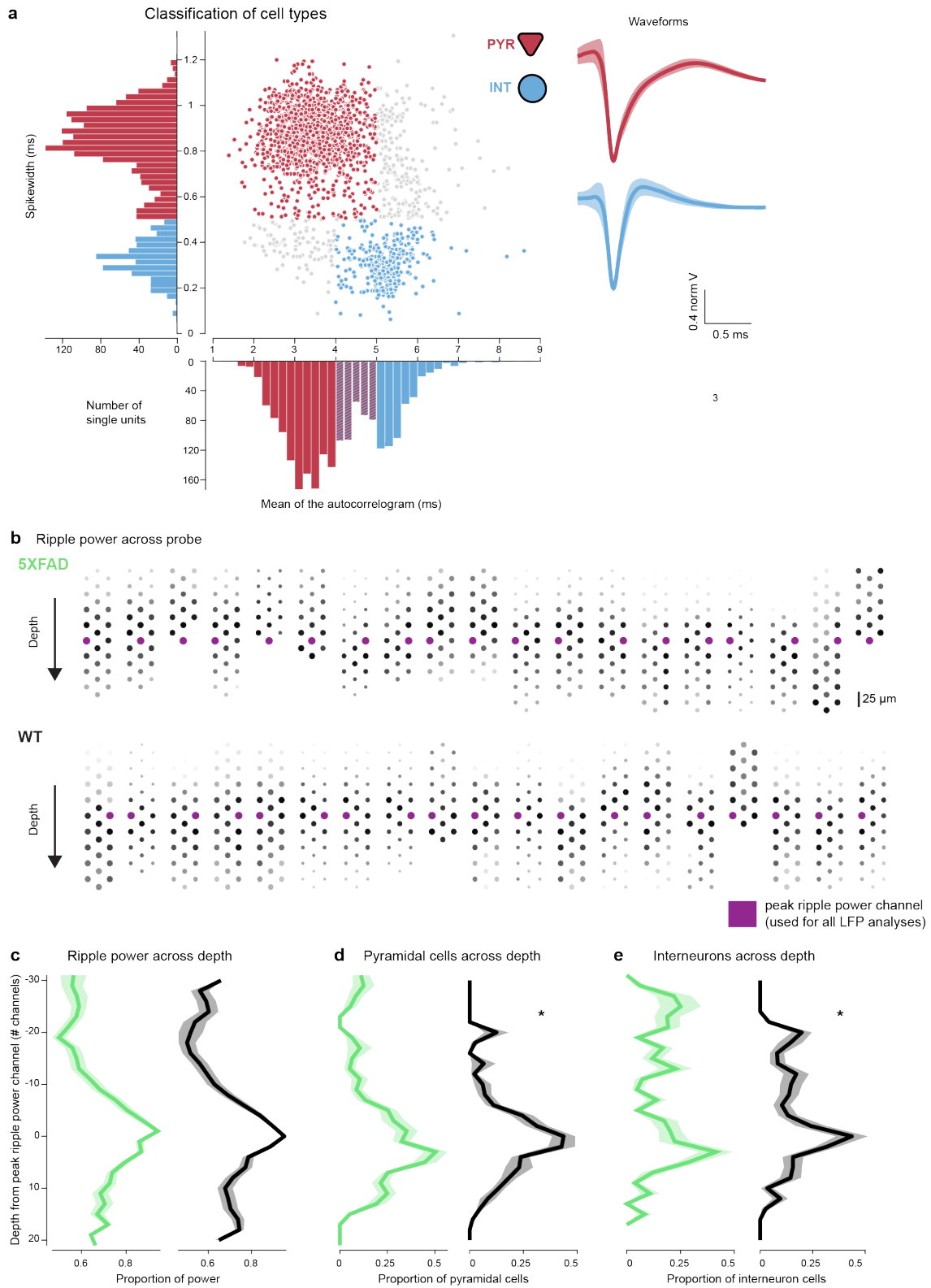


**Figure S2. Recording locations and classification of putative pyramidal cells and interneurons. Related to Figures 2-5.**

- A.** Spike width and mean of the autocorrelogram distributions for all recorded single units with putative pyramidal cells in red and putative interneurons in blue. Each point is a single unit. For histograms, color indicates how cells in this part of the distribution were classified. Inset, *right*, shows average waveforms with standard deviation (shaded) of the classified pyramidal cells and interneurons.
  - B.** *Top*, Sharp-wave ripple power across 32-channel NeuroNexus recording electrodes in *5XFAD* mice. Darker color and larger circles indicate higher sharp-wave ripple power (150-250 Hz), purple channel indicates the channel with the highest sharp-wave ripple power and is the channel used in all LFP analyses. *Bottom*, same as top in *WT* mice.
  - C.** Average proportion of sharp-wave ripple power across recording depth (linearized probe channels), centered by channel with peak sharp-wave ripple power in *5XFAD* (green) and *WT* (black) mice, mean  $\pm$  SEM..
  - D.** Average proportion of pyramidal cells across recording depth, centered by peak ripple power channel in *5XFAD* (green) and *WT* (black) mice. *5XFAD*:  $-3.62 \pm 7.64 \mu\text{m}$ ,  $n = 708$  *WT*:  $-15.75 \pm 6.53 \mu\text{m}$ ,  $n = 580$  cells.  $\text{Prob}(WT \geq 5XFAD) = 0.016 *$ , *5XFAD*: distance from center ( $\mu\text{m}$ ) percentiles = [-125 -25 50 112.5 250], *WT*: distance from center ( $\mu\text{m}$ ) percentiles = [-125 -25 0 75 175].
  - E.** As in **D** for interneurons. *5XFAD*:  $54.95 \pm 20.89 \mu\text{m}$ ,  $n = 187$  cells, *WT*:  $21.66 \pm 23.05 \mu\text{m}$ ,  $n = 146$  cells.  $\text{Prob}(WT \geq 5XFAD) = 0.0058 *$ , *5XFAD*: distance from center ( $\mu\text{m}$ ) percentiles = [-125 -37.5 -12.5 25 275], *WT*: distance from center ( $\mu\text{m}$ ) percentiles = [-137.5 -50 -12.5 12.5 150].
- All percentiles are min, 25<sup>th</sup> percentile, median, 75<sup>th</sup> percentile, max

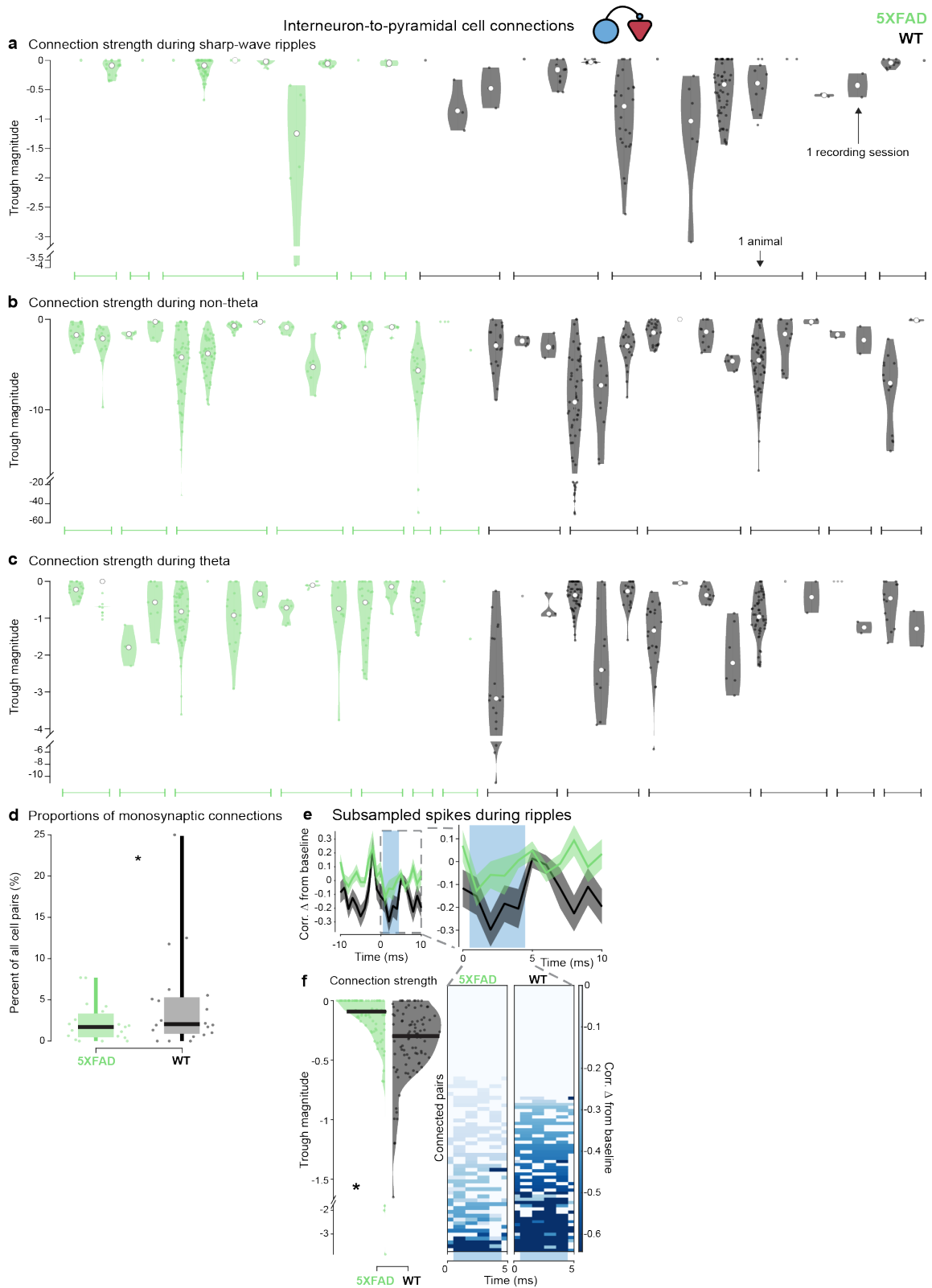


**Figure S3. Interneuron-to-pyramidal cell connection strength for individual animals and percent connections. Related to Figure 2.**

- A.** Interneuron-to-pyramidal (INT-to-PYR) cell connection strength during sharp-wave ripples for individual recording sessions in *5XFAD* (green) and *WT* (black) mice. Each data point is the connection strength of an INT-to-PYR cell pair across all sharp-wave ripple periods. Each violin plot represents a single recording session, white dots indicate median, and the bars along the x-axis indicate all recording sessions belonging to a single animal. Sessions with no putatively connected INT-to-PYR cell pairs with spiking during sharp-wave ripple periods were excluded from the plot.
- B.** As in **A** during non-theta periods.
- C.** As in **A** during theta periods.
- D.** Proportion of INT-to-PYR monosynaptic connections out of all cell pairs in *5XFAD* (green) and *WT* (black) mice. Boxplot indicates quartiles, whiskers indicate range, and black line indicates median of distribution. Each individual data point represents a single recording session. Of pairs of cells that had enough spikes to detect potential monosynaptic connections, INT-to-PYR connections accounted for  $2.21\% \pm 0.46\%$  and  $4.44\% \pm 2.34\%$  of pairs in *5XFAD* and *WT* mice, respectively.  $\text{Prob}(WT \geq 5XFAD) = 0.98^*$ , *5XFAD*:  $n = 19$  sessions, proportion of connections percentiles = [0, 0.49, 1.71, 3.10, 7.70], *WT*:  $n = 20$  sessions, proportion of connections percentiles = [0, 0.94, 2.05, 5.21, 25.00].
- E.** Example of subsampled results from monosynaptic connection strength analysis that controlled for total spike count numbers between *5XFAD* and *WT* mice by subsampling spikes from connected pair spike trains. A randomly selected subsampled iteration is shown; subsampling was repeated 50 times. The results for the other subsampling approach removing INT-to-PYR connected pairs were as follows: *5XFAD*:  $-0.14 \pm 0.13$  trough magnitude,  $n = 146$  cell pairs, *WT*:  $-0.34 \pm 0.20$  trough magnitude,  $n = 65$  cell pairs,  $\text{prob}(5XFAD \geq WT) = 0.9534$ , bootstrap test. *Left*, Average cross-correlogram of monosynaptically connected INT-to-PYR cell pairs between *5XFAD* (green) and *WT* (black) mice during sharp-wave ripple periods from -10 to +10 ms lags normalized by geometric mean firing rate and displayed as difference from baseline, mean  $\pm$  SEM. *Right*, zoomed in view of average cross-correlogram on *left* from 0 to 10s lag. Light blue box indicates region where connection strength was measured. Inhibitory connection strength was measured as the minimum value in the 1-4ms window. We rectified any positive peak values to zero to correct for pairs that likely did not fire enough spikes or were too noisy during the periods we analyzed. We found similar results when we excluded these pairs entirely. These cross-correlograms that were rectified for the strength measurement are not included in the visualization of the average and individual cross-correlograms. Statistics described in **F**.
- F.** *Left*, Example of subsampled results to control for spike counts as in **E**. Connection strengths as measured by trough magnitude in *5XFAD* and *WT* mice during sharp-wave ripple periods were averaged across 50 random subsampling iterations. Each dot indicates the connection strength measured from a single INT-to-PYR cell pair across all non-theta periods. *Right*, individual cross-correlograms of putative INT-to-PYR cell connected pairs during sharp-wave ripple periods that make up the average shown above in **E**. Heat map indicates change in correlation from baseline measurement. Note cross-correlograms during sharp-wave ripples look more variable because there are fewer spikes during-sharp wave ripples than during non-theta and theta periods. The number of spikes included in this figure was 42,065 in *5XFAD* mice and 41,227 in *WT* mice. *5XFAD*:  $-0.22 \pm 0.078$  trough magnitude, *WT*:  $-0.35 \pm 0.13$  trough magnitude.  $\text{Prob}(5XFAD \geq WT) = 0.988^*$ , here  $5XFAD \geq WT$  indicates a deficit in inhibition because inhibitory troughs are negative, *5XFAD*:  $n = 79$  INT-to-PYR cell pairs, connection strength percentiles = [-3.86 -0.24 -0.09 0 0], *WT*:  $n = 87$  INT-to-PYR cell pairs, connection strength percentiles = [-1.65 -0.48 -0.30 -0.14 0].
- All percentiles are min, 25<sup>th</sup> percentile, median, 75<sup>th</sup> percentile, max

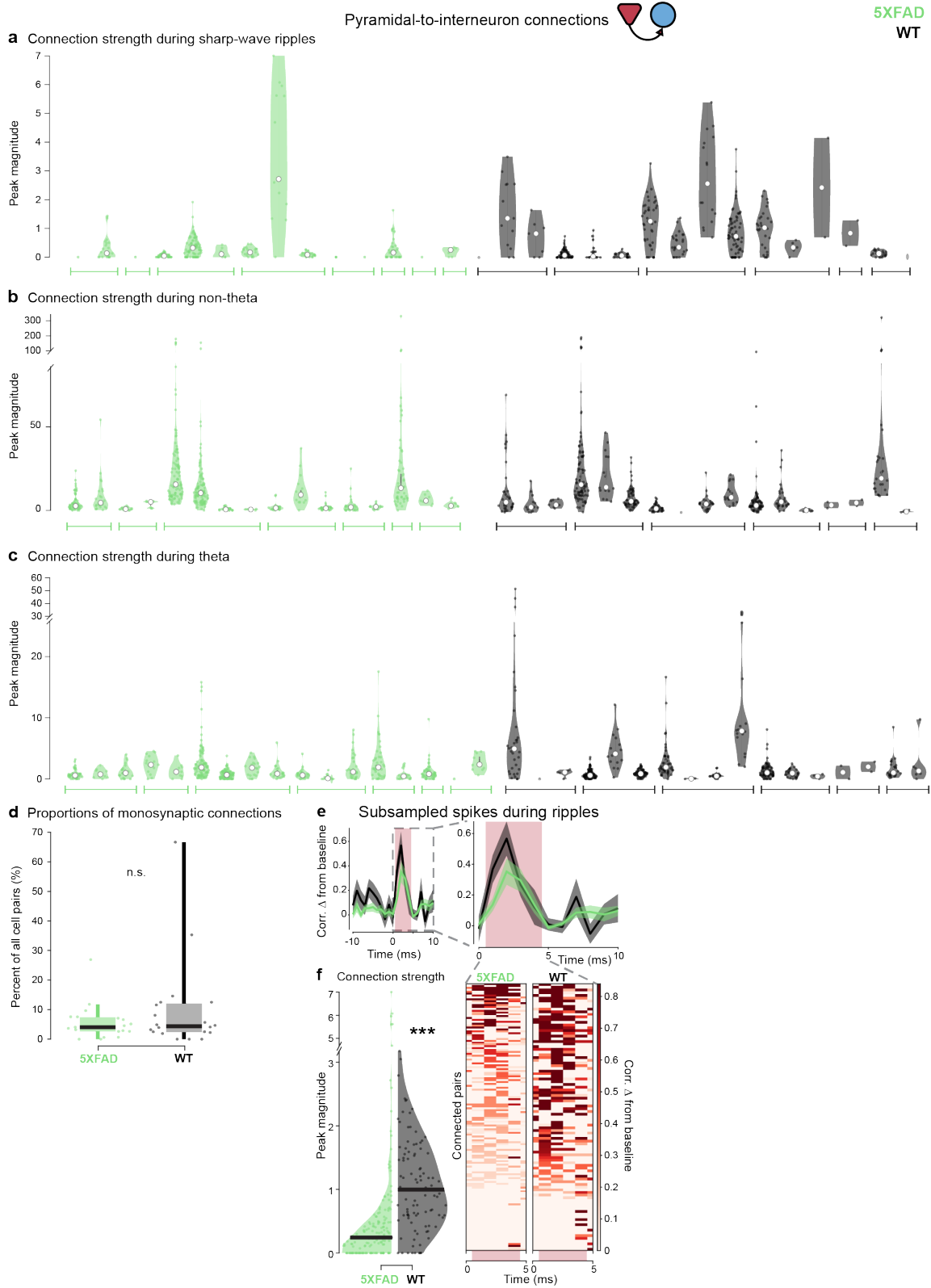


**Figure S4. Pyramidal-to-interneuron connection strength for individual animals and percent connections. Related to Figure 3.**

- A.** Pyramidal-to-interneuron (PYR-to-INT) cell connection strength during sharp-wave ripples for individual recording sessions in *5XFAD* (green) and *WT* (black) mice. Each data point is the connection strength of a PYR-to-INT pair across all sharp-wave ripple periods. Each violin plot represents a single recording session, and the bars along the x-axis indicate all recording sessions belonging to a single animal.
- B.** As in **A** for during non-theta periods.
- C.** As in **A** during theta periods.
- D.** Proportion of PYR-to-INT monosynaptic connections out of all cell pairs in *5XFAD* (green) and *WT* (black) mice. Boxplot indicates quartiles, whiskers indicate range, and black line indicates median of distribution. Each individual data point represents a single recording session. Of pairs of cells that had enough spikes to detect potential monosynaptic connections, we found that on average  $5.64\% \pm 0.78\%$  were putative PYR-to-INT connections in *5XFAD* mice, and  $9.84\% \pm 6.04\%$  of cell pairs were PYR-to-INT connections in *WT* mice.  $\text{Prob}(WT \geq 5XFAD) = 0.93$ , *5XFAD*:  $n = 19$  sessions, proportion of connections percentiles = [0, 2.64, 4.05, 7.33, 26.92], *WT*:  $n = 20$  sessions, proportion of connections percentiles = [0, 2.41, 4.37, 11.81, 66.67].
- E.** Example of subsampled results from monosynaptic connection strength analysis that controlled for total spike count numbers between *5XFAD* and *WT* mice by subsampling spikes from connected pair spike trains. A randomly selected subsampled iteration is shown; subsampling was repeated 50 times. The results for the other subsampling removing PYR-to-INT connected pairs were as follows: *5XFAD*:  $0.36 \pm 0.28$  peak magnitude,  $n = 306$  cell pairs, *WT*:  $0.62 \pm 0.23$  peak magnitude,  $n = 166$  cell pairs,  $\text{prob}(WT \geq 5XFAD) = 0.9221$ . *Left*, Average cross-correlogram of monosynaptically connected PYR-to-INT cell pairs between *5XFAD* (green) and *WT* (black) mice during sharp-wave ripple periods from -10 to +10 ms lags. Normalized by geometric mean firing rate and displayed as difference from baseline, mean  $\pm$  SEM. *Right*, view of average cross-correlogram on *left* from 0 to 10 ms lag. Light pink box indicates region where connection strength was measured. Excitatory connection strength was measured as the maximum value in the 1-4ms window. Statistics described in **F**.
- F.** *Left*, Example of subsampled results to control for spike counts as in **E**. Connection strengths as measured by peak magnitude in *5XFAD* and *WT* mice during sharp-wave ripple periods were averaged across 50 random subsampling iterations. Each dot indicates the connection strength measured from a single PYR-to-INT cell pair across all sharp-wave ripple periods. *Right*, individual cross-correlograms of putative PYR-to-INT cell connected pairs during sharp-wave ripple periods. The individual cross-correlograms make up the average shown above in **E**. Heat map indicates change in correlation from baseline measurement. Note cross-correlograms during sharp-wave ripples look more variable because there are significantly fewer spikes during-sharp wave ripples than during non-theta and theta periods. The number of spikes included in this figure was 96,736 in *5XFAD* mice and 95,871 in *WT* mice. *5XFAD*:  $0.57 \pm 0.36$  peak magnitude, *WT*:  $1.08 \pm 0.17$  peak magnitude.  $\text{Prob}(WT \geq 5XFAD) = 0.9988$  \*\*\*, *5XFAD*:  $n = 162$  PYR-to-INT cell pairs, connection strength percentiles = [0 0 0.25 0.52 7.0], *WT*:  $n = 98$  INT-to-PYR cell pairs, connection strength percentiles = [0 0.59 1.0 1.57 3.18].
- All percentiles are min, 25<sup>th</sup> percentile, median, 75<sup>th</sup> percentile, max

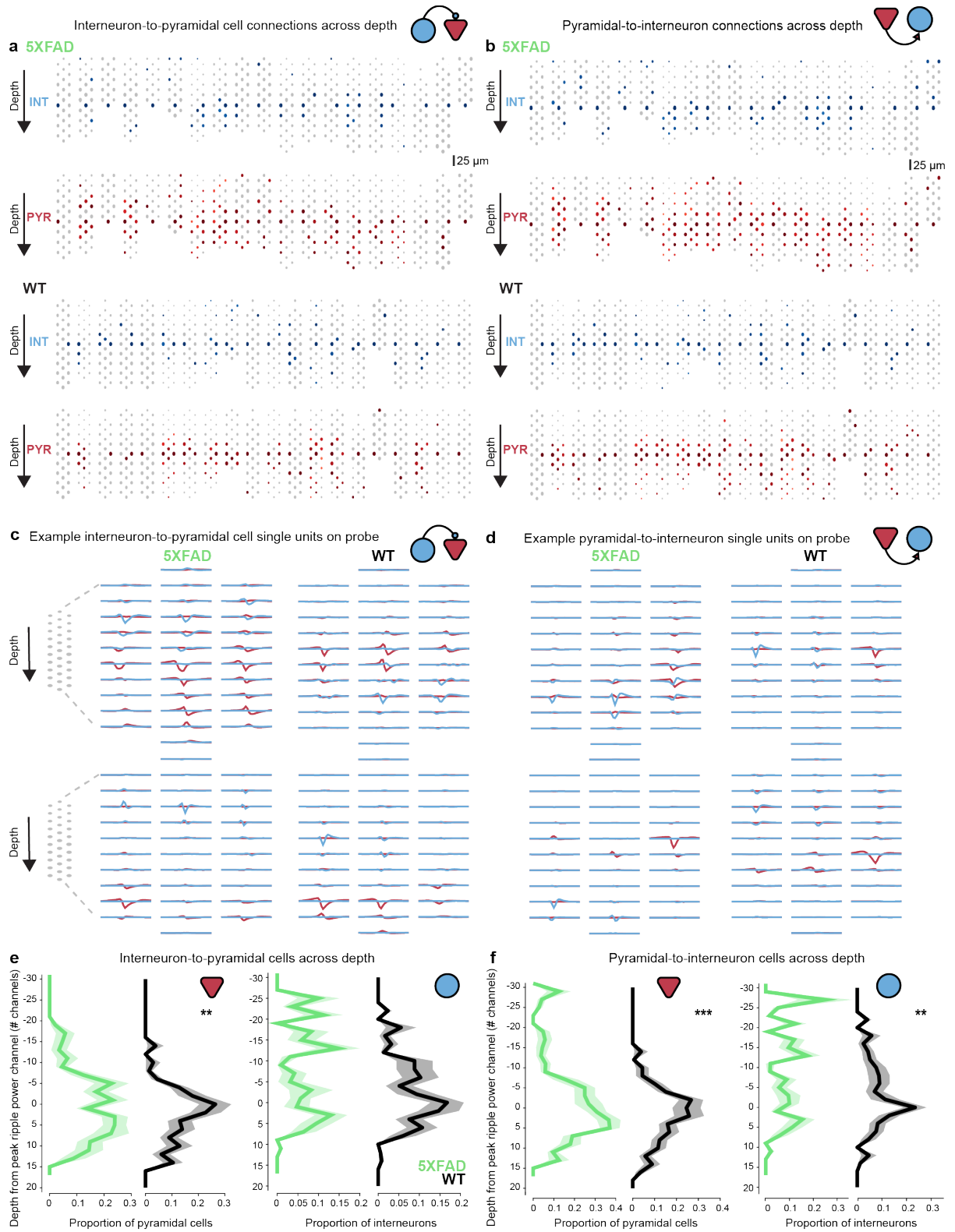


**Figure S5. Distribution of monosynaptically connected cell pairs across the electrode. Related to Figures 2-3.**

- A.** Distribution across 32-channel NeuroNexus probe of putative pyramidal cells and interneurons that are part of monosynaptically connected interneuron-to-pyramidal cell pairs in *5XFAD* mice, centered by the peak sharp-wave ripple power channel. Dot size indicates ripple power relative to the peak ripple channel. Darker color indicates larger proportion of single units, blue indicates interneurons, red indicates pyramidal cells. We examined the distribution of pyramidal cells and interneurons that were part of monosynaptically connected pairs relative to the center of the pyramidal layer as measured by the peak ripple power channel of the recording probe.
- B.** As in **A** for pyramidal-to-interneuron cell pairs.
- C.** Examples of average waveforms across 32-channel NeuroNexus probe of putative pyramidal cells and interneurons that are part of monosynaptically connected interneuron-to-pyramidal cell pairs in *5XFAD* (left) and *WT* (right) mice. Blue indicates interneurons, red indicates pyramidal cells.
- D.** As in **C** for pyramidal-to-interneuron cell pairs.
- E.** Distributions of putative pyramidal cells and interneurons that are part of monosynaptically connected interneuron-to-pyramidal cell pairs across recording depth. *Left*, Average proportion of putative pyramidal cells out of all pyramidal cells across recording depth, centered by peak sharp-wave ripple power channel in *5XFAD* (green) and *WT* (black) mice. *5XFAD*:  $-3.98 \pm 6.90 \mu\text{m}$ ,  $n = 176$  cells, *WT*:  $-19.49 \pm 8.15 \mu\text{m}$ ,  $n = 161$ .  $\text{Prob}(WT \geq 5XFAD) = 0.0017^{**}$ , *5XFAD*: distance from center ( $\mu\text{m}$ ) percentiles = [-112.5 -37.5 -6.25 25 150], *WT*: distance from center ( $\mu\text{m}$ ) percentiles = [-125 -50 -12.5 12.5 112.5]. We controlled for these differences and found similar results for deficits in inhibitory connection strengths (see **Methods**). *Right*, As in **C** for interneurons. *5XFAD*:  $46.30 \pm 22.94 \mu\text{m}$  from peak ripple channel,  $n = 54$  cells, *WT*:  $14.62 \pm 22.32 \mu\text{m}$ ,  $n = 59$  cells.  $\text{Prob}(WT \geq 5XFAD) = 0.028^{+}$ , *5XFAD*: distance from center ( $\mu\text{m}$ ) percentiles = [-100 -25 25 112.5 200], *WT*: distance from center ( $\mu\text{m}$ ) percentiles = [-125 -25 0 56.25 175].
- F.** As in **E** for pyramidal-to-interneuron cell pairs. *Left*, Average proportion of putative pyramidal cells out all pyramidal cells across recording depth, centered by peak sharp-wave ripple power channel in *5XFAD* (green) and *WT* (black) mice. *5XFAD*:  $1.91 \pm 9.72 \mu\text{m}$ ,  $n = 308$  cells, *WT*:  $-18.25 \pm 7.56 \mu\text{m}$ ,  $n = 252$  cells.  $\text{Prob}(WT \geq 5XFAD) = 0.0001^{***}$ , *5XFAD*: distance from center ( $\mu\text{m}$ ) percentiles = [-112.5 -37.5 0 25 237.5], *WT*: distance from center ( $\mu\text{m}$ ) percentiles = [-137.5 -50 -12.5 12.5 112.5]. *Right*, As in **C** for interneurons. *5XFAD*:  $56.11 \pm 22.11 \mu\text{m}$ ,  $n = 88$  cells, *WT*:  $13.97 \pm 20.44 \mu\text{m}$ ,  $n = 68$  cells.  $\text{Prob}(WT \geq 5XFAD) = 0.0025^{**}$ , *5XFAD*: distance from center ( $\mu\text{m}$ ) percentiles = [-100 -25 43.75 112.5 225], *WT*: distance from center ( $\mu\text{m}$ ) percentiles = [-125 -25 0 53.13 175].
- All percentiles are min, 25<sup>th</sup> percentile, median, 75<sup>th</sup> percentile, max

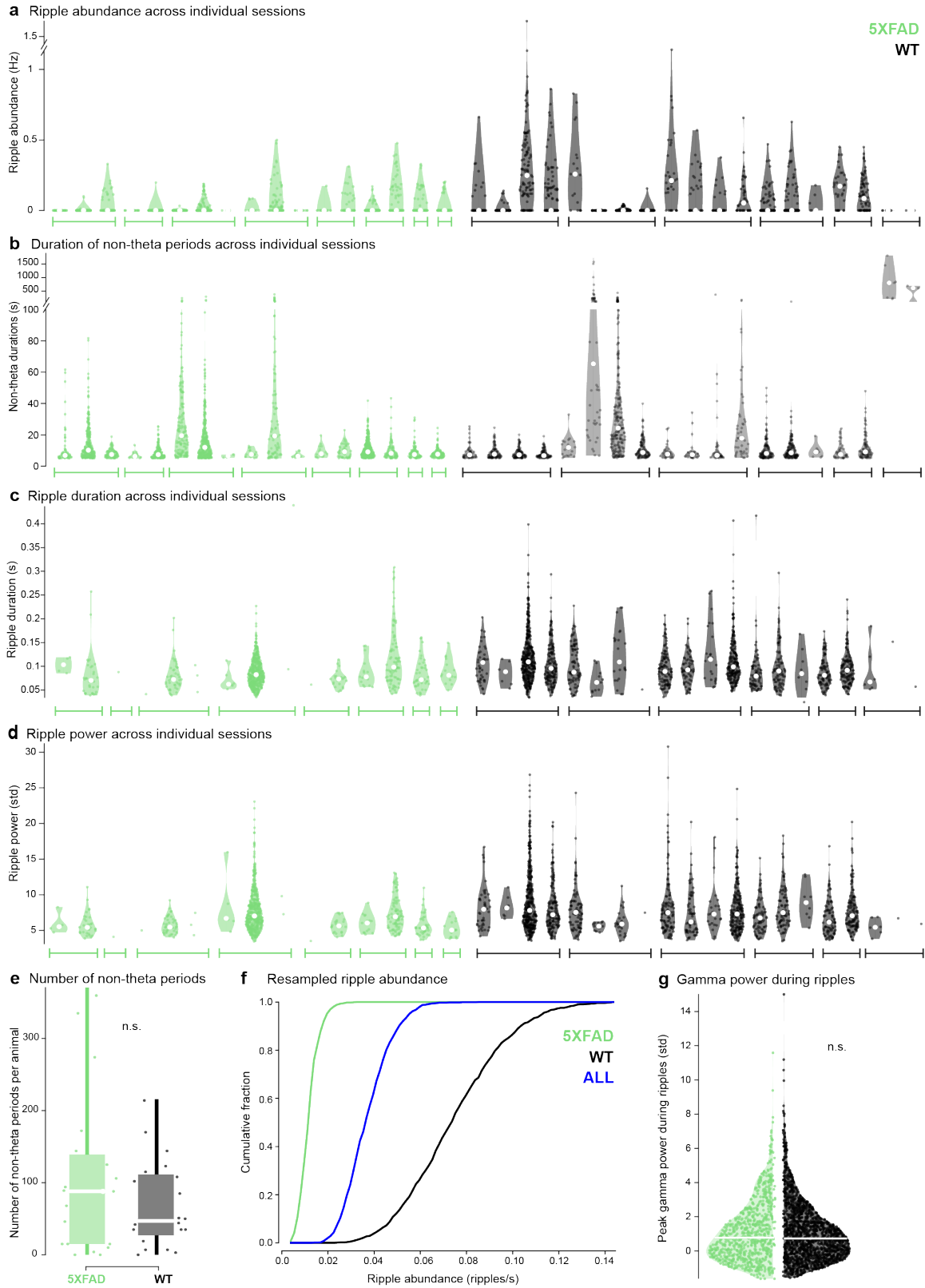


**Figure S6. Ripple abundance, duration, and power per recording and resampled distributions. Related to Figure 4.**

- A. Abundance of sharp-wave ripple events during non-theta periods longer than five seconds in *5XFAD* (green) and *WT* (black) mice by individual recording sessions. Each data point represents a non-theta period. White dots indicate median of distribution. Each violin plot represents a single recording session, and the bars along the x-axis indicate all recording sessions belonging to a single animal. We also controlled for the potential of poor ripple detection by excluding sessions with fewer than 10 SWR events, and we found that *5XFAD* mice still had significantly lower SWR abundance (*5XFAD*:  $0.020 \pm 0.011$  SWR abundance,  $n = 1252$  non-theta periods five seconds or longer, *WT*:  $0.093 \pm 0.047$  SWR abundance  $n = 1097$  non-theta periods five seconds or longer,  $\text{prob}(WT \geq 5XFAD) > 0.9999$  (limit due to resampling  $10^4$  times), bootstrap test).
- B. Duration of non-theta periods five seconds or longer for individual recording sessions in *5XFAD* (green) and *WT* (black) mice. Each data point represents a non-theta period.  $\text{Prob}(WT \geq 5XFAD) = 0.9811$ , *5XFAD*:  $n = 1969$  non-theta periods, duration of non-theta periods percentiles = [5.00, 6.47, 9.06, 14.93, 375.47], *WT*:  $n = 20$  sessions, duration of non-theta periods percentiles = [5, 6.50, 8.95, 16.16, 1815.09].
- C. Duration of sharp-wave ripple events in *5XFAD* (green) and *WT* (black) mice by individual recording sessions. Each data point represents a sharp-wave ripple event. Each violin plot represents a single recording session, and the bars along the x-axis indicate all recording sessions belonging to a single animal. White dots indicate median of distribution. Violin plot outlines (but not the individual data points) were removed for sessions with 3 or fewer data points.
- D. Standardized power of sharp-wave ripple events in *5XFAD* (green) and *WT* (black) mice by individual recording sessions. Each data point represents a sharp-wave ripple event. White dots indicate median of distribution.
- E. Number of non-theta periods greater than five seconds long for individual recording sessions in *5XFAD* (green) vs *WT* (black) mice. Each data point represents a single recording session. White line indicates median of distribution. *5XFAD*:  $103.63 \pm 43.39$  periods per session, *WT*:  $69.45 \pm 20.27$  periods per session.  $\text{Prob} = 0.078$ , *5XFAD*:  $n = 19$  sessions, number of non-theta periods percentiles = [0, 15, 88, 134.5, 369], *WT*:  $n = 20$  sessions, number of non-theta periods percentiles = [0, 31, 47, 109.75, 214].
- F. Resampled distributions of abundance of sharp-wave ripple events during non-theta periods longer than five seconds from hierarchical bootstrapping within *5XFAD* (green) and *WT* (black) groups versus across *all* (blue) groups. These results show that resampling from within each group is very different than resampling across groups, which would not be the case if there was no difference between the *5XFAD* and *WT* groups.
- G. When analyzing z-scored gamma power during SWRs, we found the strength of gamma was not different in the remaining SWRs of the *5XFAD* animals compared to the *WT* littermates. Z-scored peak slow gamma power (20-50 Hz) of sharp-wave ripple events in *5XFAD* (green) and *WT* (black) for all sessions. White line indicates median of distribution. *5XFAD*:  $1.15 \pm 0.80$  z-scored power,  $n = 776$  sharp-wave ripples, *WT*:  $1.11 \pm 0.34$  z-scored power,  $n = 1542$  sharp-wave ripples,  $\text{prob}(WT \geq 5XFAD) = 0.53$ .

All percentiles are min, 25<sup>th</sup> percentile, median, 75<sup>th</sup> percentile, max

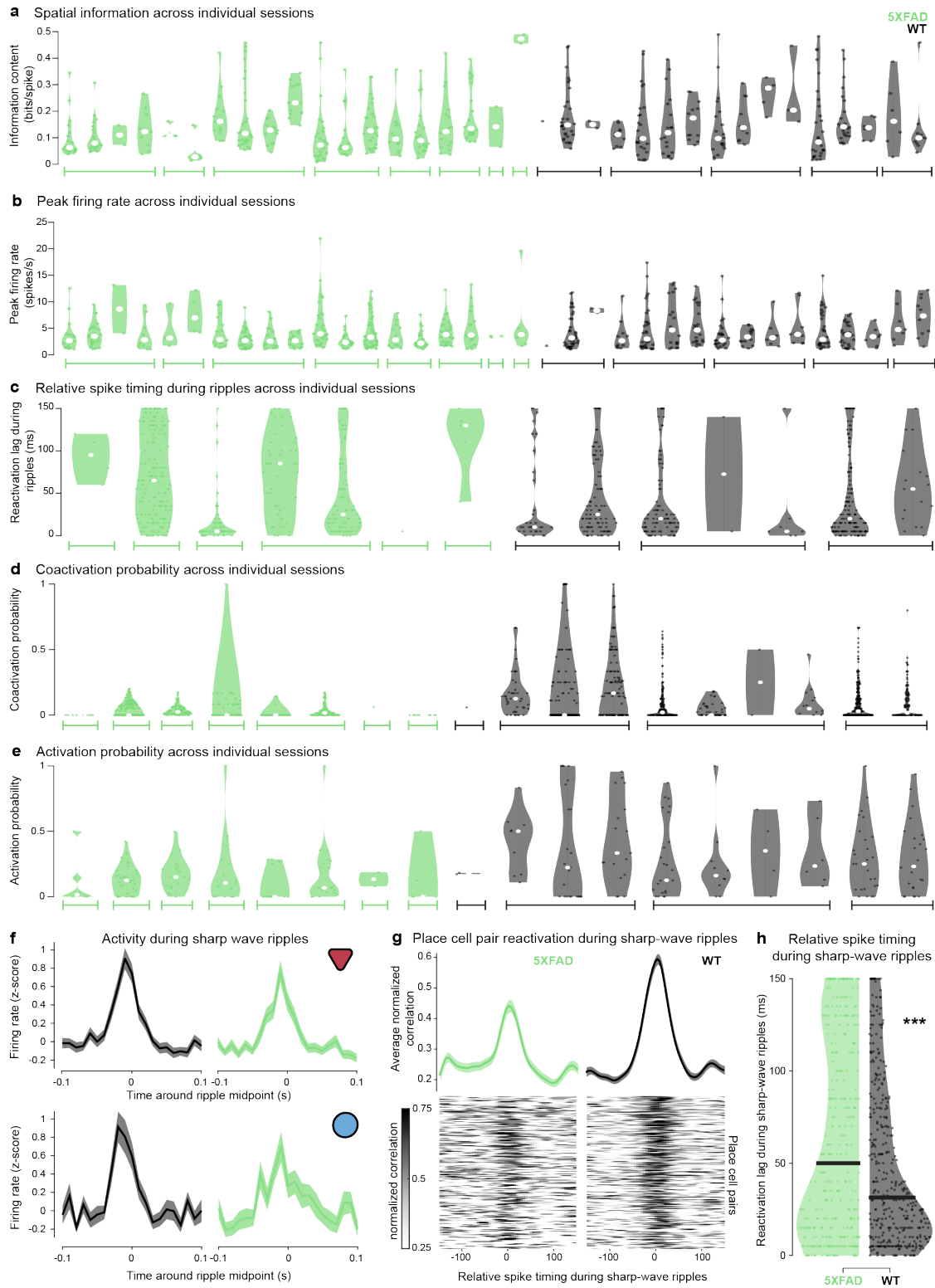


**Figure S7. Place cell properties and place cell pair reactivation during sharp-wave ripples for individual sessions. Related to Figure 5.**

- A.** Individual recording session distributions of spatial information of place cells with spatially tuned firing in the task in *5XFAD* (green) and *WT* (black) mice. Each data point represents a place cell. Each violin plot represents a single recording session, and the bars along the x-axis indicate all recording sessions belonging to a single animal. White dots indicate median of distribution. Sessions with no place cells are not shown.
- B.** Individual recording session distributions of peak firing rate of place cells with spatially tuned firing in the task in *5XFAD* and *WT* mice. Each data point represents a place cell.
- C.** Reactivation lag (or relative spike timing) of place cell pairs during sharp-wave ripples in *5XFAD* (green) and *WT* (black) mice for individual recording sessions. Reactivation lag was measured as the peak relative spike timing during sharp-wave ripples. Each data point represents the reactivation lag of a place cell pair during all sharp-wave ripple events. Each violin plot represents a single recording session, and the bars along the x-axis indicate all recording sessions belonging to a single animal. Sessions with fewer than 10 sharp-wave ripple events were excluded from the analysis. When we included all sessions we saw similar results.
- D.** Coactivation probabilities of place cell pairs during sharp-wave ripples in *5XFAD* (green) versus *WT* (black) mice for individual recording sessions. Each data point represents the coactivation probability of a place cell pair during all sharp-wave ripple events. Sessions with fewer than 10 sharp-wave ripple events were excluded from the analysis. Sessions with no co-active place cell pairs are also not shown here.
- E.** Activation probabilities of place cell pairs during sharp-wave ripples in *5XFAD* (green) versus *WT* (black) mice for individual recording sessions. Each data point represents the activation probability of a place cell during all sharp-wave ripple events. Sessions with fewer than 10 sharp-wave ripple events were excluded from the analysis.
- F.** *Top left*, putative pyramidal cell firing activity during sharp-wave ripples in *5XFAD* (green) vs *WT* (black) mice, centered around ripple midpoint, mean  $\pm$  SEM. *Top right*, peak z-scored firing rate of pyramidal cells during sharp-wave ripples. Each data point represents the z-scored firing rate of a single pyramidal cell across all sharp-wave ripple events. *5XFAD*:  $2.11 \pm 0.44$  probability, *WT*:  $2.35 \pm 0.49$  probability,  $\text{Prob}(WT \geq 5XFAD) = 0.75$ , *5XFAD*:  $n = 237$  pyramidal cells, z-scored firing rate percentiles = [-0.59 -0.18 1.95 3.85 7.68], *WT*:  $n = 266$  pyramidal cells, z-scored firing rate percentiles = [-0.74 -0.13 2.32 3.93 7.68]. *Bottom left*, interneuron cell firing activity during sharp-wave ripples in *5XFAD* (green) vs *WT* (black) mice, centered around ripple midpoint, mean  $\pm$  SEM. *Bottom right*, peak z-scored firing rate of interneurons during sharp-wave ripples. Each data point represents the z-scored firing rate of a single pyramidal cell across all sharp-wave ripple events. *5XFAD*:  $1.89 \pm 0.32$  probability, *WT*:  $1.96 \pm 0.57$  probability  $\text{Prob}(WT \geq 5XFAD) = 0.62$ , *5XFAD*:  $n = 81$  interneurons, z-scored firing rate percentiles = [-0.33 0.74 1.93 2.93 5.39], *WT*:  $n = 94$  interneurons, z-scored firing rate percentiles = [-0.46 -0.13 1.78 3.49 7.68]. We also found the firing rates of putative pyramidal cells and interneurons did not differ during non-theta and theta periods (non-theta periods *5XFAD*:  $1.85 \pm 0.89$  Hz,  $n = 627$  pyramidal cells, *WT*:  $2.14 \pm 0.36$  Hz,  $n = 519$  pyramidal cells,  $\text{prob}(WT \geq 5XFAD) = 0.90$  *5XFAD*:  $7.90 \pm 1.45$  Hz,  $n = 163$  interneurons, *WT*:  $7.96 \pm 2.22$  Hz,  $n = 135$  interneurons,  $\text{prob}(WT \geq 5XFAD) = 0.54$  bootstrap test; theta periods *5XFAD*:  $1.85 \pm 0.33$  Hz,  $n = 593$  pyramidal cells, *WT*:  $2.11 \pm 0.33$  Hz,  $n = 460$  pyramidal cells,  $\text{prob}(WT \geq 5XFAD) = 0.89$  *5XFAD*:  $8.52 \pm 1.70$  Hz,  $n = 169$  interneurons, *WT*:  $9.99 \pm 2.59$  Hz,  $n = 126$  interneurons,  $\text{prob}(WT \geq 5XFAD) = 0.87$  data not shown).
- G.** Example output of place cell reactivation analysis controlling for spike numbers between *5XFAD* and *WT* mice by subsampling spikes from place cell pair spike trains so that the final spike counts are more similar. The averages and heatmaps demonstrate one random subsampling, which was repeated 50 times to get an average relative spike timing during sharp-wave ripples for each cell pair. Reactivation during sharp-wave ripple events of place cell pairs with spiking near in time during theta in *5XFAD* and

*WT* mice. For the other subsampling approach of removing place cell pairs, the results were as follows: *5XFAD*:  $59.99 \pm 7.36$  ms,  $n = 334$  place cell pairs, *WT*:  $43.42 \pm 6.47$  ms,  $317 =$  place cell pairs,  $\text{prob}(WT \geq 5XFAD) = 0.0003$ . *Bottom*, heat maps of normalized cross-correlograms of place cell pairs during sharp-wave ripples with spiking near in time during theta (lower half of the activity index of all place cell pairs). *Top*, average of all place cell pair reactivation during sharp-wave ripple events with spiking near in time during theta.

- H.** Relative spike timing during sharp-wave ripples in place cells were averaged across 50 random subsampling iterations. Since the *5XFAD* group was not subsampled, these reactivation lag values follow discrete time bins versus the *WT* group which were averages of 50 discrete time bin values for each place cell pair from the subsampling analysis. Relative spike timing during sharp-wave ripples in place cells that spike near in time during theta in *5XFAD* (green) and *WT* (black) mice. Each dot indicates the peak reactivation lag of a single place cell pair across all sharp-wave ripple events. The number of spikes included in this figure was 107,412 in *5XFAD* mice and 107,232 in *WT* mice. Black bar indicates median of distribution. *5XFAD*:  $64.15 \pm 7.03$  ms, *WT*:  $47.96 \pm 4.89$  ms.  $\text{Prob}(WT \geq 5XFAD) = 0.0001$  (limit due to resampling  $10^4$  times) \*\*\*, *5XFAD*:  $n = 335$  place cell pairs, spike timing lags during ripples percentiles = [0 15 50 120 150], *WT*:  $n = 385$ , spike timing lags during ripples percentiles = [0 10 31.40 79.2 150].

All percentiles are min, 25<sup>th</sup> percentile, median, 75<sup>th</sup> percentile, max